HHS Public Access
Author manuscript
Leukemia. Author manuscript; available in PMC 2019 May 03.

Published in final edited form as:
Leukemia. 2019 May ; 33(5): 1135–1147. doi:10.1038/s41375-018-0269-8.

Mlh1 deficiency increases the risk of hematopoietic malignancy after simulated space radiation exposure.

Rutulkumar Patel[1], **Luchang Zhang**[1], **Amar Desai**[7], **Mark J. Hoenerhoff**[3], **Lucy H. Kennedy**[3], **Tomas Radivoyevitch**[4], **Yuguang Ban**[5], **Xi Steven Chen**[5,6], **Stanton L. Gerson**[7], and **Scott M. Welford**[5,8]

[1]Department of Pharmacology, Case Western Reserve University, Cleveland, OH

[2]Department of Medicine, Case Western Reserve University, Cleveland, OH

[3]In Vivo Animal Core Unit for Laboratory Animal Medicine, University of Michigan, MI

[4]Department of Quantitative Health Sciences, Cleveland Clinic, Cleveland, OH

[5]Sylvester Comprehensive Cancer Center, University of Miami, Miami FL

[6]Department of Public Health Sciences, University of Miami, Miami FL

[7]Case Comprehensive Cancer Center, Case Western Reserve University, Cleveland, OH

[8]Department of Radiation Oncology, University of Miami, Miami, FL

Abstract

Cancer-causing genome instability is a major concern during space travel due to exposure of astronauts to potent sources of high-linear energy transfer (LET) ionizing radiation. Hematopoietic stem cells (HSCs) are particularly susceptible to genotoxic stress, and accumulation of damage can lead to HSC dysfunction and oncogenesis. Our group recently demonstrated that aging human HSCs accumulate microsatellite instability coincident with loss of *MLH1*, a DNA Mismatch Repair (MMR) protein, which could reasonably predispose to radiation-induced HSC malignancies. Therefore, in an effort to reduce risk uncertainty for cancer development during deep space travel, we employed an *Mlh1*$^{+/-}$ mouse model to study the effects high-LET ^{56}Fe ion space-like radiation. Irradiated *Mlh1*$^{+/-}$ mice showed a significantly higher incidence of lymphomagenesis with ^{56}Fe ions compared to γ-rays and unirradiated mice, and malignancy correlated with increased MSI in the tumors. In addition, whole exome sequencing analysis revealed high SNVs and INDELs in lymphomas being driven by loss of *Mlh1* and frequently mutated genes had a strong correlation with human leukemias. Therefore, the data suggest that age-related MMR deficiencies could lead to HSC malignancies after space radiation, and that countermeasure strategies will be required to adequately protect the astronaut population on the journey to Mars.

Competing Interests
The authors declare there are no competing financial interests.

This research was funded by NASA grant NNX14AC95G. Authors also declare no conflicts of interest.

Introduction

The success of manned missions to outer space depends on many factors, including overcoming health risks such as space radiation. Space radiation is composed of protons and high (H) atomic number (Z) and energy (E) (HZE) charged ions that arise from Solar Particle Events (SPEs), Galactic Cosmic Radiation (GCR), and the Van Allen radiation belts [1–3]. In particular, GCR is composed of 90% of protons, 9% of alpha particles (^{4}He nuclei), and ~1% nuclei of HZE particles such as ^{12}C, ^{16}O, ^{20}Ne, ^{24}Mg, ^{26}Al, ^{28}Si, and ^{56}Fe ions [4, 5]. These particles have a broad range of LET characteristics (densities of induced ionization events along particle tracks). The extent to which differences in LET relate to different types of health risks remains largely unknown, and current mitigation strategies and shielding materials are ineffective to protect astronauts from HZE radiation due to the penetrance of the particles. In addition, there is incomplete understanding of the radiobiology of HZE particles and a lack of accurate risk assessment models, which puts future human-based space missions in question.

A major space radiation-induced health risk to astronauts is tumorigenesis. Cancer fatality risk prediction is an important consideration for deep space missions for government agencies including the National Aeronautics and Space Administration (NASA). Data for low-LET radiation-induced cancer risk in humans come from epidemiological studies of Japanese A-bomb survivors, radiotherapy patients, and occupational radiation workers [6]; while data for high-LET radiation rely mostly animal modeling. Various studies performed using mice have identified cancers such as mammary tumors, hepatocellular carcinoma, colorectal cancer, and leukemia as being HZE-induced [7–9]. The data show clear differences between high- and low-LET radiation, both in tumor type and incidence. Radiation-induced lymphomas and leukemia represent a significant concern for astronauts during space travel due to the efficiency of radiation induced hematopoietic malignancies.

Ionizing radiation (IR) produces a variety of DNA damage products that are repaired by multiple DNA damage response (DDR) processes. The DNA mismatch repair (MMR) pathway is part of the DDR that fixes mismatches generated by DNA polymerase during replication, but also repairs base damage from a variety of stresses including radiation [10, 11]. In particular, MMR eliminates IR-induced buildup of 8-oxoguanine lesions to prevent adenine misincorporation during DNA replication [12–14]. MMR defects in tumors are associated with microsatellite instability (MSI) – gain or loss of nucleotides from microsatellite tracks in DNA. MSI is classically associated with colorectal cancers where loss of functional MMR components is frequently found, and tumor cells are said to display a mutator phenotype indicating the lack of a key caretaker pathway [15, 16]. MMR could thus play a radioprotective tumor suppressor role, a concept supported by studies that have shown enhanced induction of intestinal carcinogenesis in MMR defective mice exposed to oxidative stress [17], and others that have found induction of a preleukemic state in HSCs [18]. MMR consists of seven different proteins, including *MLH1*, which is crucial for bringing repair machinery to mismatch repair sites. Studies have found epigenetic silencing of *MLH1* in cancers such as glioblastoma multiforme, endometrial, lung, and head and neck squamous carcinomas [19–22]. Therefore, loss of *MLH1* may predispose cells to become cancerous, particularly if exposed to high-LET ionizing radiation.

A recent study by our group demonstrated that MSI accumulates in human HSCs as a function of age, with loss of *MLH1* by promoter hypermethylation [23, 24]. Given that upper end of astronauts are ~46 years old, HSCs with deficient MMR function will likely be exposed to space radiation. We thus sought to characterize the interaction between loss of *MLH1* and exposure to high-LET radiation in the induction of hematopoietic malignancies. Using *Mlh1*$^{+/-}$ mice, that exhibit MSI [25], exposed to 100 or 250 cGy of low-LET γ-rays and 10 or 100 cGy of high-LET ^{56}Fe ion particles, we find that *Mlh1* status does not have an impact on long-term HSC function. However, *Mlh1* allelic deficiency significantly increases the risk of hematopoietic malignancy after γ-ray or ^{56}Fe ion radiation with associated loss of *Mlh1* function determined by high levels of single nucleotide variants (SNVs)/insertions and deletions (INDELs) in resulting tumors.

Materials and Methods

Animals

Institutional Animal Care and Use Committee approved protocols were followed at Case Western Reserve University (CWRU) and Brookhaven National Laboratory (BNL). The *Mlh1*$^{+/-}$ strain B6.129-Mlh1^{tm1Rak}/NCI was acquired from the National Cancer Institute at Frederick [25]. All animals were bred and maintained at the CWRU Animal Research Core. All mice had *ad libitum* access to food (Laboratory Rodent Diet 5LOD, Lab Diet, St. Louis, MO) and water. The animal housing room was maintained on a 12:12h light:dark cycle and constant temperature (72 ± 2° F).

Particle irradiation

Adult B6.129-Mlh1^{tm1Rak} male and female mice (~12 weeks) were shipped to BNL roughly one week prior to irradiation. The animals were divided into 10 groups of ~ 40 animals to obtain statistical power, including sham-irradiated *Mlh1*$^{+/+}$ and *Mlh1*$^{+/-}$. On the day of exposure, animals were arranged into an animal pie-shaped holder and placed perpendicular to a 20×20 cm beam line to expose with 10 or 100 cGy of 600 MeV/n ^{56}Fe ions at a dose rate of 5–50 cGy/minute. Additional animals were exposed to 100 or 250 cGy of γ-rays in a Shepherd Mark I irradiator-containing ^{137}Cs at BNL. Bone marrow (BM) cells were irradiated at NSRL for clonogenic survival assays and competitive repopulation assays. *Mlh1*$^{+/+}$ and *Mlh1*$^{+/-}$ mice (5 animals per genotype) were sacrificed on site, and bone marrow cells were harvested and irradiated with 0, 10, 50, 100, or 250 cGy of 600 MeV/n ^{56}Fe ions. Additional BM cells were irradiated with 0, 10, 50, 100, or 250 cGy of γ-rays.

Clonogenic survival assay

Irradiated *Mlh1*$^{+/+}$ and *Mlh1*$^{+/-}$ BM cells were plated with complete methylcellulose media (MethoCult™ GF M3434 or MethoCult™ M3630, STEMCELL Technologies) to measure survival by colony forming unit (CFU) assay. M3434 media was used for myeloid colony formation, and M3630 media for pre-B lymphoid assays. All assays were performed twice with three replicates (50,000 cells/plate for myeloid CFU and 250,000 cells/plate for lymphoid CFU), and counted between 7–14 days post-plating.

Competitive repopulation assay

Three million irradiated or sham-irradiated whole BM cells from *Mlh1*$^{+/+}$ or *Mlh1*$^{+/-}$ mice (CD45.2) were mixed with whole BM cells of age matched wild type mice (CD45.1) at a 1:1 ratio and injected via tail vein into lethally irradiated (1100 cGy) CD45.1 recipient mice. Blood was collected via the submandibular vein at 4-week and at 10-week time points post bone marrow transplant (BMT) and analyzed by flow cytometry to measure CD45.2 positive cells in the peripheral blood.

Histology and Immunohistochemistry

Animals were euthanized at first signs of morbidity and tumors were collected. All tumors were fixed in 10% formaldehyde for 24 hours followed by immersion into 70% ethanol until processed and sectioned. Hematoxylin and eosin (H&E) stains were performed and then analyzed at the In Vivo Animal Core facility at the University of Michigan. Selected lymphomas were further analyzed by immunohistochemistry (IHC) with B220 (BD Pharmingen # 550286), CD3 (Thermo Fisher # RM9107), or F4/80 (Abd Serotec # MCA497RT) antibodies.

Microsatellite instability

Tumors were assessed for four mononucleotide repeats (*mBat-26, mBat-37, mBat-59,* and *mBat-64*) [26]. Amplification of each mononucleotide repeat was performed separately by PCR. Detection of amplified PCR fragments was performed on an Agilent TapeStation and analyzed by TapeStation Analysis Software A.02.01 SR1. Each marker length (deletion or addition of nucleotides) measured by the software was compared to marker length of a normal tissue to identify each marker as being stable or unstable. The classification of microsatellite instability was accomplished by calculating the number of unstable markers for each tumor sample. We classified tumors as MSI stable, low, or high based on numbers of these markers with instabilities being 0/4, 1/4, or >1/4, respectively.

Whole-exome sequencing

Whole-exome sequencing (WES) was carried out by using a Truseq Exome library prep kit according to manufacturer's protocol, and a 2×75bp HS run was performed using an Illumina HiSeq2500. Sequencing quality was assessed using FastQC (ver.11.5). Trimmomatic (ver.0.32) was used to remove sequence adapters and low quality leading and trailing bases from reads [27]. Filtered and trimmed reads were aligned to reference genome mm10 using the Burrows-Wheeler Aligner (ver.0.7.12) algorithm [28]. Refinement of reads alignment was performed using GATK (ver.3.4.0) analysis toolkit, including PCR duplicated removal, local INDEL realignment, and base recalibration [29]. For variant calling, we performed individual tumor sample calling using Mutect2, against the sample from normal mouse tissue as normal reference [30]. Final SNVs and INDELs were selected with stringent criteria and final variants were annotated using VariantAnnotation (ver. 1.20.3) R package [31]. Data are deposited in SRA at NCBI (accession #PRJNA487630)

Results

Mlh1 heterozygosity significantly increases high-LET radiation induced malignancy.

Knockout animals are known to be tumor prone, and thus do not phenocopy aged people; in contrast, *Mlh1*$^{+/-}$ animals exhibit relatively low spontaneous tumorigenesis in spite of partial loss of MMR function [32]. During follow-up, mice were euthanized at the onset of signs of morbidity or the appearance of visible tumors (figure 1A). We found a significant reduction in tumor-free survival of *Mlh1*$^{+/-}$ mice irradiated with 100 or 250 cGy of γ-ray *vs*. sham-irradiated *Mlh1*$^{+/-}$ mice or irradiated *Mlh1*$^{+/+}$ mice ($p<0.0001$, figure 1B) Interestingly, we observed significantly increased mortalities in *Mlh1*$^{+/-}$ mice exposed to 10 or 100 cGy ^{56}Fe ions *vs*. sham-irradiated *Mlh1*$^{+/-}$ or irradiated *Mlh1*$^{+/+}$ mice ($p<0.0001$, figure 1C). Indeed, the biological impact of 100 cGy of ^{56}Fe ions exceeded 100 cGy of γ-rays ($p=0.0470$). In addition, *Mlh1*$^{+/-}$ mice exposed to 100 cGy ^{56}Fe ion IR showed a significant lower tumor free survival compared to mice exposed to 10 cGy ^{56}Fe ion IR ($p=0.0456$). In contrast, we observed no significant increases in tumorigenesis of *Mlh1*$^{+/+}$ mice regardless of the type of radiation used. To gain insight into the time of onset of disease, the same data with exposed animals grouped by genotype were used to estimate 70% survival times: sham-irradiated *Mlh1*$^{+/-}$ mice, 513 days; *Mlh1*$^{+/-}$ mice irradiated with 100 or 250 cGy of γ-rays, 446 and 444 days; *Mlh1*$^{+/-}$ mice irradiated with 10 or 100 cGy of ^{56}Fe ion irradiation, 424 and 385 days; and all *Mlh1*$^{+/+}$ mice, regardless of being irradiated, time not reached (figures 1D–1F, supplementary table 1). Thus, loss of *Mlh1* enhances radiation-induced tumorigenesis that heavily depends on radiation quality.

Mlh1 deficiency increases the incidence of lymphomagenesis after low and high LET radiation.

Loss of *Mlh1* is associated with a higher incidence of lymphomas and gastrointestinal tumors in animal models [33, 34]. Therefore, we next examined tumors collected from *Mlh1*$^{+/+}$ and *Mlh1*$^{+/-}$ mice by hematoxylin and eosin staining to determine tumor types and if radiation exposure altered the distribution of tumor types formed. Histopathology analysis revealed different tumor types, but lymphoma was found to be the most common tumor (figure 2A). Sporadic age-related tumors such as hepatocellular adenomas (HCA), hepatocellular carcinomas (HCC), histiocytic sarcoma (HS), and other rare tumors (figure 2B–2F; supplementary table 2) were also observed. The analysis determined that ~40% of total tumors found in *Mlh1*$^{+/+}$ cohorts were lymphomas (figure 2G). Interestingly, we observed a significant difference in tumor type distribution between *Mlh1*$^{+/+}$ mice treated or not with low- or high-LET radiation ($p=0.0447$). In contrast, ~80% of tumors of *Mlh1*$^{+/-}$ cohorts were lymphomas (figure 2H). Further, *Mlh1*$^{+/-}$ cohorts revealed significantly higher incidence of multiple tumors per mouse compared to *Mlh1*$^{+/+}$ cohorts ($p=0.0288$, figure 2I). These data argue that *Mlh1* deficiency increases incidence mostly of hematopoietic malignancies after IR, independent of radiation quality (i.e. LET).

Mlh1$^{+/-}$ cohorts have higher incidence of T-cell rich B-cell lymphomas.

Lymphomas are classified by immunophenotype. The majority of lymphomas show immune cell infiltrates in the tumor microenvironment, which is associated with profound influence on disease pathology [35]. Therefore, we decided to further explore the lymphomas based on

IHC analysis. We used CD3, B220, and F4/80 to discern T cell, B cell, and macrophage/histiocytes in the tumors, respectively. Staining patterns revealed six different types of lymphoma that include T-cell rich B-cell (TRB) lymphoma, B-cell lymphoma, T-cell lymphoma, histiocytic sarcoma, B/T mixed lymphoma, and T-cell/histiocyte rich B-cell lymphoma (figure 3A–3F; supplementary table 3). We found 40–60% of lymphomas were TRB lymphomas in the *Mlh1*$^{+/+}$ mice (figure 3G). Interesting, we observed roughly 30% of lymphomas were histiocytic sarcoma in sham-irradiated and γ-irradiated *Mlh1*$^{+/+}$ mice, whereas no histiocytic sarcomas were found in ^{56}Fe particle irradiated *Mlh1*$^{+/+}$ mice. Similarly, we observed that the majority of lymphomas were TRB lymphomas in all treatment groups of *Mlh1*$^{+/-}$ mice (figure 3H). Collectively, the data show that TRB lymphomas were common in *Mlh1*$^{+/+}$ and *Mlh1*$^{+/-}$ mice regardless of radiation type and that infiltrating T-cells might play a role in the process of lymphomagenesis.

Mlh1$^{+/-}$ tumors exhibit elevated levels of microsatellite instability.

Loss of MMR strongly correlates with MSI in many human cancers [36], and we anticipated that mononucleotide repeats would be highly susceptible to MSI in *Mlh1*$^{+/-}$ tumors compared to *Mlh1*$^{+/+}$ tumors, particularly because heterozygosity of *Mlh1* has been shown to associate with decreased DNA repair [23, 25]. The average sizes of four mononucleotide markers were measured from MMR-proficient control samples and shown as peak values in figures 4A–4D. MSI analysis showed that a majority of markers had a deletion of one or more nucleotides in the stretch of mononucleotide repeats in *Mlh1*$^{+/}$− tumors (figure 4E–4H). We found that roughly 80% of *Mlh1*$^{+/-}$ tumors showed high MSI, while only 2% of these tumors showed stable MSI. In contrast, we found that roughly 45% of *Mlh1*$^{+/+}$ tumors were high MSI, and that 55% were either stable or low MSI. Thus, MSI differed in *Mlh1*$^{+/+}$ *vs.* *Mlh1*$^{+/-}$ tumors (p=0.0048, figure 4I). Interestingly, we observed no change in high MSI of *Mlh1*$^{+/-}$ tumors by different radiation types, including sham-irradiated (figure 4J). Collectively, the data show that MSI associates with tumorigenesis in both the *Mlh1* wild type and heterozygous mice, and hence MMR status could be a potential risk stratification marker for individuals exposed to high LET ionizing radiation.

Significantly elevated levels of SNVs and INDELs appear in *Mlh1*$^{+/-}$ lymphomas.

MMR deficiency is associated with a mutator phenotype. In particular, loss of *Msh2* and *Mlh1*, key components of MMR, have been shown to increase mutational frequency in newborn mice and during different stages of embryogenesis [37, 38]. After verifying high MSI in *Mlh1* heterozygous tumors, we decided to further analyze TRB lymphomas by WES to study SNV/INDEL patterns in wildtype vs heterozygous lymphomas. The WES analysis revealed a significant increase in mutation rate of *Mlh1*$^{+/-}$ compared to *Mlh1*$^{+/+}$ TRB lymphomas arising from sham-, γ-rays, or ^{56}Fe ion IR (p<0.0001, figure 5A, 5B). Surprisingly, radiation exposure showed no further increase in number of SNVs of irradiated cohorts compared to sham-irradiated cohorts, regardless of *Mlh1* status (p=0.9225, figure 5A,5B). In addition, WES analysis showed significantly higher INDELs in the *Mlh1*$^{+/-}$ irradiated cohorts compared to *Mlh1*$^{+/+}$ irradiated cohorts (p=0.0314, figure 5A, 5C). The data suggest that *Mlh1* heterozygosity was associated with higher SNVs, while INDELs were correlated with irradiation plus loss of *Mlh1*.

For further analysis, we identified frequently mutated genes in *Mlh1*$^{+/+}$ and *Mlh1*$^{+/-}$ cohorts based on type of radiation exposure. To examine the role of recurring mutations occurred at specific loci, we defined a gene as frequently mutated if it was found to be mutated in ≥ 40% of at least one cohort. The analysis revealed that a significantly higher number of frequently mutated genes were found in *Mlh1*$^{+/-}$ cohorts compared to *Mlh1*$^{+/+}$ cohorts of TRB lymphomas ($p<0.0001$, figure 5F, 5G). *Mlh1* heterozygosity not only increased the mutation rate, but the repeated nature of mutations occurring at the same loci suggests importance of these genes in tumorigenesis. In fact, we compared frequently mutated genes to well-defined cancer causing genes and discovered that ~13% of the genes in each cohort of *Mlh1*$^{+/-}$ TRB lymphomas were associated with cancer (supplementary table 4). Collectively, WES analysis not only revealed higher SNVs and INDELs in *Mlh1*$^{+/-}$ TRB lymphomas, but also that mutations occurred frequently in genes responsible for tumorigenesis.

High LET radiation induces a unique spectrum of genetic alterations in genes associated with human leukemia.

The C57BL/6 mouse model is a useful resource for studying radiation-induced cancers if parallels can be drawn between the mechanisms of radiation-induced tumorigenesis of mouse lymphomas and human leukemias. Many studies have shown that expression changes in genes such as *Ikaros*, *Bcl11b*, and *Epha7* occur in both mouse lymphomas and various types of human leukemias [39–42]. Therefore, we asked whether genes frequently mutated in TRB lymphomas are relevant to human leukemia, and whether ^{56}Fe ions produced unique mutations compared to γ-rays. We identified 8 and 39 recurrently altered human leukemia genes in *Mlh1*$^{+/+}$ and *Mlh1*$^{+/-}$ TRBs, respectively (figure 6A, 6B). Interestingly, irradiated cohorts showed different gene mutational patterns compared to sham-IR tumors, suggesting a distinct pathway leading to lymphomagenesis. For instance, high rates of somatic mutations in *Cbl*, *Huwe1*, *Runx1*, and *Ttn* genes were found in all *Mlh1*$^{+/-}$ cohorts. In contrast, some genes were found mutated in specific treatment groups: *Jag1*, *Kit*, *Nup214*, and *Pik3cd* were prominently found mutated in the sham-IR cohort; *Dnmt3a* and *Myb* were prominently found in γ-ray cohort; and *Myc* was only found in ^{56}Fe ion IR cohort. In addition, the majority of the mutations were nonsynonymous in nature (figure 6C). Thus sequence analyses of TRB lymphomas suggests that common mechanisms underlie these mouse lymphomas and radiation induced human leukemias, and strengthens the position that *MLH1* defects will predispose space radiation-exposed astronauts to disease development.

Discussion

The impact of age-associated MMR defects to the risk of space radiation-induced malignancies has not been previously assessed. The current study provides evidence that loss of *Mlh1* in HSCs, which occurs as a function of age in normal healthy individuals [23] leads to a significantly higher incidence of tumorigenesis after exposure to high LET radiation, and that the incidence is dependent on the type of radiation exposure. At the same time, we observed no significant changes in acute hematopoietic functions of *Mlh1*$^{+/-}$ vs *Mlh1*$^{+/+}$ BM cells measured by CFU and competitive repopulation assays (supplementary figure 1). Further, long-term differentiation potential of HSCs was also unaffected by *Mlh1* status (supplementary figure 2). Thus, the critical observation described here is that MMR

defective animals are cancer prone when exposed to cosmic radiation. *Mlh1*$^{+/-}$ mice show increased incidence of lymphomagenesis compared to *Mlh1*$^{+/+}$ mice, and MSI is coincident with tumorigenesis in all cohorts. WES analysis of the tumors revealed a significantly higher rate of SNVs/INDELs in *Mlh1* haploinsufficient TRB lymphomas along with strong evidence of recurrent gene mutations occurring in carcinogenic and leukemogenic genes. The data are in agreement with the observation that MMR deficiency due to *Msh2* loss has been shown to promote a preleukemic state without affecting HSC repopulation function [18]. Together, our studies demonstrate that low- and high-LET radiation induce elevated tumorigenesis in *Mlh1* deficient contexts that could alter the risk paradigm for astronauts on deep space missions.

After high-LET iron particle exposure, nearly all energy deposition occurs in confined regions of the cell near the particle track and associated δ-ray penumbras, causing dense local ionization and clustered DNA lesions [43, 44]. Thus, the likelihood of repair of DNA damage and survival of cells is significantly reduced for most cell types following the same doses of high-LET compared to low-LET irradiation. In our studies, we observed a significantly higher impact of high-LET ^{56}Fe particles on HSC acute functions compared to low-LET γ-rays, regardless of *Mlh1* status. Similarly, we found that radiation exposure significantly accelerated tumorigenesis in *Mlh1*$^{+/-}$ mice compared to wild type mice, and that high LET radiation was markedly more effective. The findings are in agreement with work from the Weil group and others which showed higher incidence of tumorigenesis in animals exposed to high-LET IR compared to low-LET γ-rays exposure [8, 45–47]. *Mlh1*$^{+/-}$ mice exposed to 100 cGy ^{56}Fe ion IR were reduced to 70% survival ~130 and ~60 days earlier compared to sham-IR and 100 cGy γ-rays exposed *Mlh1*$^{+/-}$ mice, respectively. Collectively, these findings suggest that loss of *Mlh1* and high-LET radiation exposure together are responsible for not only higher frequency but early incidence of tumorigenesis.

Radiation induced damage by high-LET sources may have an indirect role in leading to tumorigenesis. Late-occurring chromosomal aberrations and global DNA methylation in hematopoietic stem/progenitor cells have been shown after ^{28}Si ion irradiation [48]. Kennedy, et al, have also observed altered methylation in bronchial epithelial cells after ^{56}Fe and ^{28}Si exposure, contributing to lung cancer, which in theory could also contribute to the mechanism of loss of MLH1 expression in HSCs[49]. Mice exposed to high-LET ^{16}O (600 MeV/n) ions showed significantly higher level of ROS in HSCs three months after irradiation, suggesting that cells experience continuous damage stress [50, 51]. Continuous ROS levels in HSCs post irradiation could lead to mutation accumulation in absence of functional MMR and may explain our observation of significantly higher SNVs in all cohorts of *Mlh1*$^{+/-}$ TRB lymphomas. However, we did not detect differences in SNVs between sham and irradiated cohorts, which may be due to the longer time taken by the sham-IR cohort to reach to 70% survival hence allowing extra time to accumulate SNVs. In addition, we discovered significantly higher mean INDEL size (≥5 and ≥10 base pairs) in all *Mlh1*$^{+/-}$ cohorts compared to *Mlh1*$^{+/+}$ cohorts, implying *Mlh1* plays a role not only in MMR but also in double strand break repair (figure 5D, 5E), which has been suggested in other models [52, 53]. Collectively, the WES analysis suggests that *Mlh1* loss is strongly associated with high mutational burden in lymphomas, and high mean INDELs size could be due to *Mlh1* involvement in repair mechanism other than MMR.

We observed not only a high mutation rate in *Mlh1* haploinsufficient lymphomas, but also frequent mutations occurring in carcinogenic loci. *Mlh1* loss is associated with frequent mutations occurring in the loci of *NF1* and *ATR* [54, 55]. Similarly, we found frequent mutations in *Nf1* and *Atr* along with 12 other carcinogenic genes (*Met, Cacna1d, Ptprd, Nbea, Gnaq, Cntnap2, Csmd3, Pabpc1, Lrp1b, Zfhx3, Dcc,* and *Ctnna2*) across all cohorts of $Mlh1^{+/-}$ TRB lymphomas. In addition, each cohort of $Mlh1^{+/-}$ TRB lymphoma showed radiation-specific gene mutational profiles. For instance, well-defined carcinogenic genes such as *Cdh1, Eps15, Was, Atp2b3, Cdh11,* and *Myc* were predominantly mutated in ^{56}Fe ion IR $Mlh1^{+/-}$ cohort while the γ-ray $Mlh1^{+/-}$ cohort revealed frequent mutations in genes such as *Ddx6, Tsc2, Raf1, Nt5c2, Crebbp, Tfe3, Stat3, Map2k1, Dnmt3a, Bcor, Map3k1*, and *Arid2*. Critically, we observed an enrichment of mutations in the $Mlh1^{+/-}$ lymphomas that also occur in human leukemias. The data also revealed radiation quality specific effects, such as the observation of *Myc* mutation exclusively in ^{56}Fe, *Myb* mutation exclusively in γ-rays, and *Nup214* mutation predominately in sham irradiated $Mlh1^{+/-}$ lymphomas. It is unclear at this point what mechanism would lead to gene-specific mutations, but the observation is similar to one recently published by Porada and colleagues when human HSCs were exposed to HZE radiation that showed enrichment in mutations in leukemia-associated genes within 24 hours of exposure [56]. Therefore, our study suggests that age-related *MLH1* loss in astronaut HSCs results in a preleukemic state that can be exacerbated by high-LET radiation exposures received during space travel.

Increased use of high-LET radiotherapy also raises concern for therapy-related malignancies in patients with MMR defects, both in the hematopoietic system and beyond. Although further studies will be required to better characterize the molecular nature of tumors formed in our studies, and what types of doses and LET are sufficient for enhancing tumor development, the results should be interpreted carefully, as astronauts in outer space may be exposed to several types of HZE particles with different fluences and energies. Future studies will be required to assess the effects of medium LET species and subsequently mixed ion beam fields and lower dose-rates to better mimic space radiation. In summary, the data suggest that loss of *Mlh1* in HSCs, either genetically or as a function of age, could play a critical role in sensitizing humans to space-radiation induced HSC malignancies. Further studies will be required to more accurately calculate risks, both for missions into outer space and for patients undergoing current proton or future carbon-ion radiotherapy.

Supplementary Material

Refer to Web version on PubMed Central for supplementary material.

Acknowledgements

This research was funded by NASA grant NNX14AC95G. The authors are grateful to all members of NASA Space Radiation Laboratory and support staff at Brookhaven National Laboratory, in particular to Adam Rusek, Chiara La Tessa, and Peter Guida, for their assistance. The authors are also thankful to shared resources of the Case Comprehensive Cancer Center including Radiation Resources, Integrated Genomics, Cytometry & Microscopy, and Hematopoietic Biorepository & Cellular Therapy. We also thank the generosity of Thomas F. Peterson, Jr.

References

1. Cucinotta FA, Schimmerling W, Wilson JW, Peterson LE, Badhwar GD, Saganti PB, et al. Space radiation cancer risks and uncertainties for Mars missions. Radiation research 2001 11; 156(5 Pt 2): 682–688. [PubMed: 11604093]
2. Edwards AA. RBE of radiations in space and the implications for space travel. Physica medica : PM : an international journal devoted to the applications of physics to medicine and biology : official journal of the Italian Association of Biomedical Physics 2001; 17 **Suppl** 1: 147–152.**Suppl**
3. Schimmerling W, Cucinotta FA, Wilson JW. Radiation risk and human space exploration. Advances in space research : the official journal of the Committee on Space Research 2003; 31(1): 27–34.
4. Heinrich W, Roesler S, Schraube H. Physics of cosmic radiation fields. Radiation protection dosimetry 1999; 86(4): 253–258. [PubMed: 11543393]
5. Chancellor JC, Scott GB, Sutton JP. Space Radiation: The Number One Risk to Astronaut Health beyond Low Earth Orbit. Life 2014 9 11; 4(3): 491–510. [PubMed: 25370382]
6. V B. Health Effects of Exposure to Low Levels of Ionizing Radiation. 1990 20140718 ISBN- 0309039959 ISBN- 0309039975.
7. Bielefeldt-Ohmann H, Genik PC, Fallgren CM, Ullrich RL, Weil MM. Animal studies of charged particle-induced carcinogenesis. Health physics 2012 11; 103(5): 568–576. [PubMed: 23032886]
8. Weil MM, Bedford JS, Bielefeldt-Ohmann H, Ray FA, Genik PC, Ehrhart EJ, et al. Incidence of acute myeloid leukemia and hepatocellular carcinoma in mice irradiated with 1 GeV/nucleon (56)Fe ions. Radiation research 2009 8; 172(2): 213–219. [PubMed: 19630525]
9. Datta K, Suman S, Kallakury BV, Fornace AJ Jr. Exposure to heavy ion radiation induces persistent oxidative stress in mouse intestine. PloS one 2012; 7(8): e42224. [PubMed: 22936983]
10. Wei K, Clark AB, Wong E, Kane MF, Mazur DJ, Parris T, et al. Inactivation of Exonuclease 1 in mice results in DNA mismatch repair defects, increased cancer susceptibility, and male and female sterility. Genes & development 2003 3 01; 17(5): 603–614. [PubMed: 12629043]
11. Iyer RR, Pluciennik A, Burdett V, Modrich PL. DNA mismatch repair: functions and mechanisms. Chemical reviews 2006 2; 106(2): 302–323. [PubMed: 16464007]
12. Fritzell JA, Narayanan L, Baker SM, Bronner CE, Andrew SE, Prolla TA, et al. Role of DNA mismatch repair in the cytotoxicity of ionizing radiation. Cancer research 1997 11 15; 57(22): 5143–5147. [PubMed: 9371516]
13. Mazurek A, Berardini M, Fishel R. Activation of human MutS homologs by 8-oxo-guanine DNA damage. The Journal of biological chemistry 2002 3 08; 277(10): 8260–8266. [PubMed: 11756455]
14. Macpherson P, Barone F, Maga G, Mazzei F, Karran P, Bignami M. 8-oxoguanine incorporation into DNA repeats in vitro and mismatch recognition by MutSalpha. Nucleic acids research 2005; 33(16): 5094–5105. [PubMed: 16174844]
15. Vilar E, Gruber SB. Microsatellite instability in colorectal cancer-the stable evidence. Nature reviews Clinical oncology 2010 3; 7(3): 153–162.
16. Kinzler KW, Vogelstein B. Cancer-susceptibility genes. Gatekeepers and caretakers. Nature 1997 4 24; 386(6627): 761, 763. [PubMed: 9126728]
17. Piao JS, Nakatsu Y, Ohno M, Taguchi K, Tsuzuki T. Mismatch Repair Deficient Mice Show Susceptibility to Oxidative Stress-Induced Intestinal Carcinogenesis. Int J Biol Sci 2014; 10(1): 73–79.
18. Qing Y, Gerson SL. Mismatch repair deficient hematopoietic stem cells are preleukemic stem cells. PloS one 2017; 12(8): e0182175. [PubMed: 28767666]
19. Ma Y, Chen Y, Petersen I. Expression and promoter DNA methylation of MLH1 in colorectal cancer and lung cancer. Pathology, research and practice 2017 4; 213(4): 333–338.
20. Gutierrez VF, Marcos CA, Llorente JL, Guervos MA, Iglesias FD, Tamargo LA, et al. Genetic profile of second primary tumors and recurrences in head and neck squamous cell carcinomas. Head & neck 2012 6; 34(6): 830–839. [PubMed: 22127891]

21. Stark AM, Doukas A, Hugo HH, Hedderich J, Hattermann K, Maximilian Mehdorn H, et al. Expression of DNA mismatch repair proteins MLH1, MSH2, and MSH6 in recurrent glioblastoma. Neurological research 2015 2; 37(2): 95–105. [PubMed: 24995467]
22. Cosgrove CM, Cohn DE, Hampel H, Frankel WL, Jones D, McElroy JP, et al. Epigenetic silencing of MLH1 in endometrial cancers is associated with larger tumor volume, increased rate of lymph node positivity and reduced recurrence-free survival. Gynecologic oncology 2017 9; 146(3): 588–595. [PubMed: 28709704]
23. Kenyon J, Fu P, Lingas K, Thomas E, Saurastri A, Santos Guasch G, et al. Humans accumulate microsatellite instability with acquired loss of MLH1 protein in hematopoietic stem and progenitor cells as a function of age. Blood 2012 10 18; 120(16): 3229–3236. [PubMed: 22740444]
24. Kenyon J, Nickel-Meester G, Qing Y, Santos-Guasch G, Drake E, PingfuFu, et al. Epigenetic Loss of MLH1 Expression in Normal Human Hematopoietic Stem Cell Clones is Defined by the Promoter CpG Methylation Pattern Observed by High-Throughput Methylation Specific Sequencing. International journal of stem cell research and therapy 2016; 3(2).
25. Edelmann W, Cohen PE, Kane M, Lau K, Morrow B, Bennett S, et al. Meiotic pachytene arrest in MLH1-deficient mice. Cell 1996 6 28; 85(7): 1125–1134. [PubMed: 8674118]
26. Bacher JW, Abdel Megid WM, Kent-First MG, Halberg RB. Use of mononucleotide repeat markers for detection of microsatellite instability in mouse tumors. Molecular carcinogenesis 2005 12; 44(4): 285–292. [PubMed: 16240453]
27. Bolger AM, Lohse M, Usadel B. Trimmomatic: a flexible trimmer for Illumina sequence data. Bioinformatics 2014 8 1; 30(15): 2114–2120. [PubMed: 24695404]
28. Li H, Durbin R. Fast and accurate short read alignment with Burrows-Wheeler transform. Bioinformatics 2009 7 15; 25(14): 1754–1760. [PubMed: 19451168]
29. DePristo MA, Banks E, Poplin R, Garimella KV, Maguire JR, Hartl C, et al. A framework for variation discovery and genotyping using next-generation DNA sequencing data. Nature genetics 2011 5; 43(5): 491-+.
30. Cibulskis K, Lawrence MS, Carter SL, Sivachenko A, Jaffe D, Sougnez C, et al. Sensitive detection of somatic point mutations in impure and heterogeneous cancer samples. Nat Biotechnol 2013 3; 31(3): 213–219. [PubMed: 23396013]
31. Obenchain V, Lawrence M, Carey V, Gogarten S, Shannon P, Morgan M. VariantAnnotation: a Bioconductor package for exploration and annotation of genetic variants. Bioinformatics 2014 7 15; 30(14): 2076–2078. [PubMed: 24681907]
32. Tokairin Y, Kakinuma S, Arai M, Nishimura M, Okamoto M, Ito E, et al. Accelerated growth of intestinal tumours after radiation exposure in Mlh1-knockout mice: evaluation of the late effect of radiation on a mouse model of HNPCC. International journal of experimental pathology 2006 4; 87(2): 89–99. [PubMed: 16623753]
33. Edelmann W, Yang K, Kuraguchi M, Heyer J, Lia M, Kneitz B, et al. Tumorigenesis in Mlh1 and Mlh1/Apc1638N mutant mice. Cancer research 1999 3 15; 59(6): 1301–1307. [PubMed: 10096563]
34. Yao X, Buermeyer AB, Narayanan L, Tran D, Baker SM, Prolla TA, et al. Different mutator phenotypes in Mlh1- versus Pms2-deficient mice. Proceedings of the National Academy of Sciences of the United States of America 1999 6 8; 96(12): 6850–6855. [PubMed: 10359802]
35. Scott DW, Gascoyne RD. The tumour microenvironment in B cell lymphomas. Nature reviews Cancer 2014 8; 14(8): 517–534. [PubMed: 25008267]
36. Hause RJ, Pritchard CC, Shendure J, Salipante SJ. Classification and characterization of microsatellite instability across 18 cancer types. Nature medicine 2016 11; 22(11): 1342–1350.
37. Fan X, Li Y, Zhang Y, Sang M, Cai J, Li Q, et al. High Mutation Levels are Compatible with Normal Embryonic Development in Mlh1-Deficient Mice. Radiation research 2016 10; 186(4): 377–384. [PubMed: 27643877]
38. He D, Chen Y, Li H, Furuya M, Ikehata H, Uehara Y, et al. Role of the Msh2 gene in genome maintenance and development in mouse fetuses. Mutation research 2012 6 1; 734(1–2): 50–55. [PubMed: 22465156]
39. Dovat S, Song C, Payne KJ, Li Z. Ikaros, CK2 kinase, and the road to leukemia. Molecular and cellular biochemistry 2011 10; 356(1–2): 201–207. [PubMed: 21750978]

40. Payne KJ, Dovat S. Ikaros and tumor suppression in acute lymphoblastic leukemia. Critical reviews in oncogenesis 2011; 16(1–2): 3–12. [PubMed: 22150303]
41. Gutierrez A, Kentsis A, Sanda T, Holmfeldt L, Chen SC, Zhang J, et al. The BCL11B tumor suppressor is mutated across the major molecular subtypes of T-cell acute lymphoblastic leukemia. Blood 2011 10 13; 118(15): 4169–4173. [PubMed: 21878675]
42. Lopez-Nieva P, Vaquero C, Fernandez-Navarro P, Gonzalez-Sanchez L, Villa-Morales M, Santos J, et al. EPHA7, a new target gene for 6q deletion in T-cell lymphoblastic lymphomas. Carcinogenesis 2012 2; 33(2): 452–458. [PubMed: 22114070]
43. Cucinotta FA, Nikjoo H, Goodhead DT. Model for radial dependence of frequency distributions for energy imparted in nanometer volumes from HZE particles. Radiation research 2000 4; 153(4): 459–468. [PubMed: 10761008]
44. Mirsch J, Tommasino F, Frohns A, Conrad S, Durante M, Scholz M, et al. Direct measurement of the 3-dimensional DNA lesion distribution induced by energetic charged particles in a mouse model tissue. Proceedings of the National Academy of Sciences of the United States of America 2015 10 06; 112(40): 12396–12401. [PubMed: 26392532]
45. Weil MM, Ray FA, Genik PC, Yu Y, McCarthy M, Fallgren CM, et al. Effects of 28Si ions, 56Fe ions, and protons on the induction of murine acute myeloid leukemia and hepatocellular carcinoma. PloS one 2014; 9(7): e104819. [PubMed: 25126721]
46. Suman S, Kumar S, Moon BH, Strawn SJ, Thakor H, Fan Z, et al. Relative Biological Effectiveness of Energetic Heavy Ions for Intestinal Tumorigenesis Shows Male Preponderance and Radiation Type and Energy Dependence in APC(1638N/+) Mice. International journal of radiation oncology, biology, physics 2016 5 1; 95(1): 131–138.
47. Wang X, Farris Iii AB, Wang P, Zhang X, Wang H, Wang Y. Relative effectiveness at 1 gy after acute and fractionated exposures of heavy ions with different linear energy transfer for lung tumorigenesis. Radiation research 2015 2; 183(2): 233–239. [PubMed: 25635344]
48. Rithidech KN, Honikel LM, Reungpathanaphong P, Tungjai M, Jangiam W, Whorton EB. Late-occurring chromosome aberrations and global DNA methylation in hematopoietic stem/progenitor cells of CBA/CaJ mice exposed to silicon ((28)Si) ions. Mutation research 2015 11; 781: 22–31. [PubMed: 26398320]
49. Kennedy EM, Powell DR, Li Z, Bell JSK, Barwick BG, Feng H, et al. Galactic Cosmic Radiation Induces Persistent Epigenome Alterations Relevant to Human Lung Cancer. Scientific reports 2018 4 30; 8(1): 6709. [PubMed: 29712937]
50. Sridharan DM, Asaithamby A, Bailey SM, Costes SV, Doetsch PW, Dynan WS, et al. Understanding cancer development processes after HZE-particle exposure: roles of ROS, DNA damage repair and inflammation. Radiation research 2015 1; 183(1): 1–26. [PubMed: 25564719]
51. Chang J, Luo Y, Wang Y, Pathak R, Sridharan V, Jones T, et al. Low Doses of Oxygen Ion Irradiation Cause Acute Damage to Hematopoietic Cells in Mice. PloS one 2016; 11(7): e0158097. [PubMed: 27367604]
52. Eccleston J, Yan C, Yuan K, Alt FW, Selsing E. Mismatch repair proteins MSH2, MLH1, and EXO1 are important for class-switch recombination events occurring in B cells that lack nonhomologous end joining. Journal of immunology 2011 2 15; 186(4): 2336–2343.
53. Chahwan R, van Oers JM, Avdievich E, Zhao C, Edelmann W, Scharff MD, et al. The ATPase activity of MLH1 is required to orchestrate DNA double-strand breaks and end processing during class switch recombination. The Journal of experimental medicine 2012 4 9; 209(4): 671–678. [PubMed: 22451719]
54. Gutmann DH, Winkeler E, Kabbarah O, Hedrick N, Dudley S, Goodfellow PJ, et al. Mlh1 deficiency accelerates myeloid leukemogenesis in neurofibromatosis 1 (Nf1) heterozygous mice. Oncogene 2003 7 17; 22(29): 4581–4585. [PubMed: 12881715]
55. Fang Y, Tsao CC, Goodman BK, Furumai R, Tirado CA, Abraham RT, et al. ATR functions as a gene dosage-dependent tumor suppressor on a mismatch repair-deficient background. The EMBO journal 2004 8 04; 23(15): 3164–3174. [PubMed: 15282542]
56. Rodman C, Almeida-Porada G, George SK, Moon J, Soker S, Pardee T, et al. In vitro and in vivo assessment of direct effects of simulated solar and galactic cosmic radiation on human hematopoietic stem/progenitor cells. Leukemia 2017 6; 31(6): 1398–1407. [PubMed: 27881872]

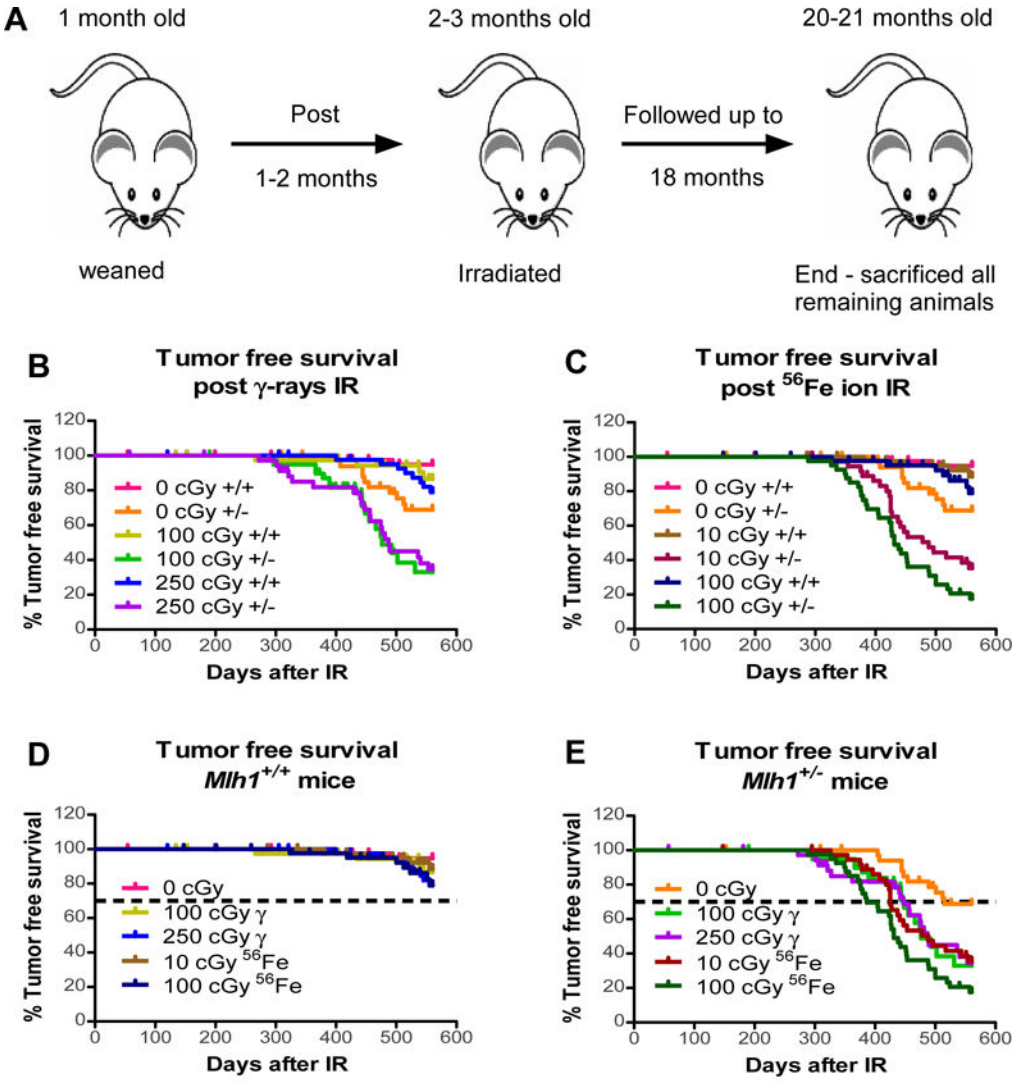

F

Treatment groups	Time to reach 70% survival (*Mlh1*$^{+/+}$ mice)	Time to reach 70% survival (*Mlh1*$^{+/-}$ mice)
0 cGy	> 560 days	513 days
100 cGy γ-rays IR	> 560 days	446 days
250 cGy γ-rays IR	> 560 days	444 days
10 cGy ^{56}Fe ion IR	> 560 days	424 days
100 cGy ^{56}Fe ion IR	> 560 days	385 days

Figure 1: Long-term tumorigenesis assay.

(A) Schematic representation of long-term tumorigenesis assay design. Tumor free survival of *Mlh1*$^{+/+}$ and *Mlh1*$^{+/-}$ mice post (B) 100 or 250 cGy γ-rays, or (C) 10 or 100 cGy ^{56}Fe ions (n=36–44, number of *Mlh1*$^{+/+}$ or *Mlh1*$^{-/-}$ mice used for each radiation exposure). (D) Tumor free survival of *Mlh1*$^{+/+}$ mice post 0, 100 or 250 cGy γ-rays, or 10 or 100 cGy ^{56}Fe ions. (E) Tumor free survival of *Mlh1*$^{+/-}$ mice post 0, 100 or 250 cGy γ-rays, or 10 or 100 cGy ^{56}Fe ions. (F) Days post-irradiation to reach 70% survival. Variance between groups is not significantly different.

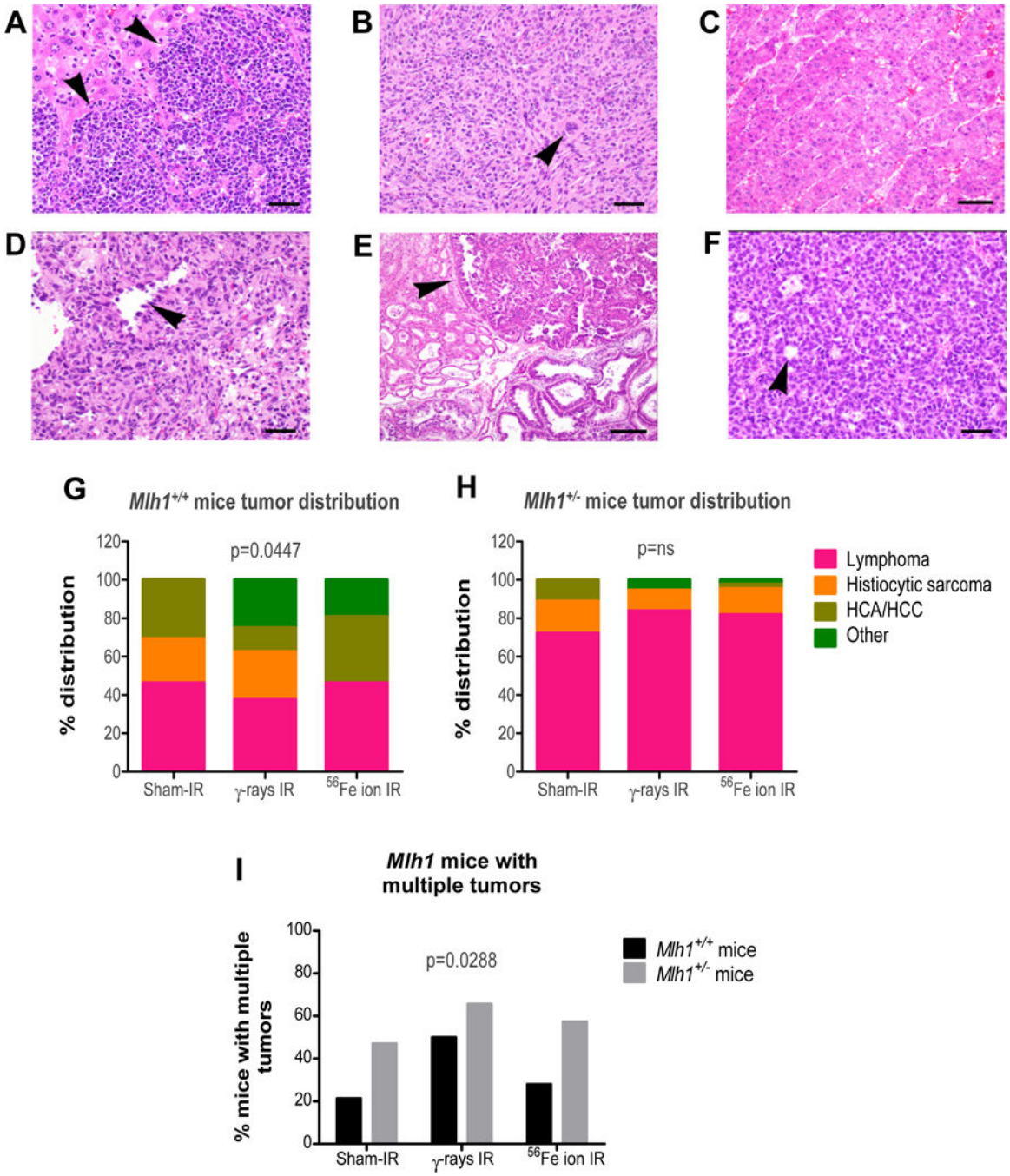

Figure 2: Histopathology of tumors from *Mlh1*$^{+/+}$ and *Mlh1*$^{+/-}$ mice.

(A) Lymphoma in sections of liver, characterized by sheets of neoplastic lymphocytes infiltrating and effacing normal hepatic parenchyma (arrowheads) (40X, bar = 20um). (B) Histiocytic sarcoma composed of round to spindyloid neoplastic cells with occasional multinucleate giant cells (arrowhead) (20X, bar = 50um). (C) Hepatocellular carcinoma composed of lobules, cords, and trabeculae of atypical hepatocytes replacing normal parenchyma (bar = 50um). (D) Hemangiosarcoma composed of sheets and bundles of spindle-shaped cells forming haphazard vascular channels (arrowhead) lined by neoplastic

endothelial cells (40X, bar = 20um). (E) Harderian gland adenoma characterized by an expansile proliferation (arrowhead) of tubules and acini of fairly well differentiated glandular epithelial cells (bar = 100um). (F) Ovarian granulosa cell tumor composed of solid lobules and nests of neoplastic cells often forming rudimentary follicular structures (arrowhead) (40X, bar = 20um). (G) Percentage tumor distribution based on histology of tumors collected from *Mlh1*$^{+/+}$ mice treated with sham-, γ-, or ^{56}Fe ion irradiation. (H) Percentage tumor distribution based on histology of tumors collected from *Mlh1*$^{+/-}$ mice treated with sham-, γ-, or ^{56}Fe ion irradiation. (I) Aggressive cancer measured by percentage of mice with multiple tumor types or same tumor type in multiple organs. Histopathology was performed on 13–27 tumors of *Mlh1*$^{+/+}$ origin and 18–44 tumors of *Mlh1*$^{+/-}$ origin. Tumor distribution was analyzed by Chi-square and multiple tumor incidence was analyzed by two-way ANOVA; ns = non-significant.

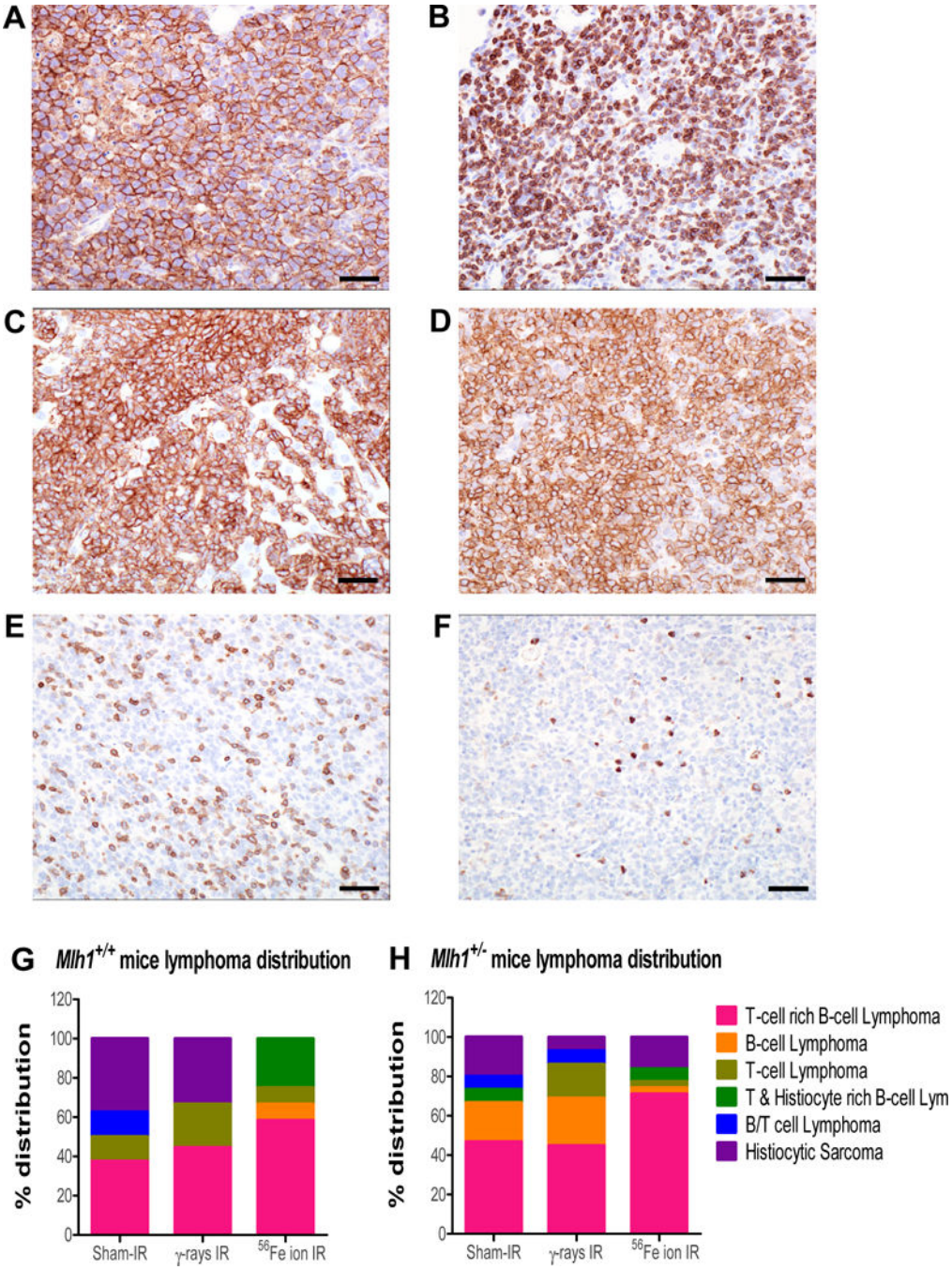

Figure 3: Immunohistochemistry of lymphomas from *Mlh1*$^{+/+}$ and *Mlh1*$^{+/-}$ mice.

(A) B-cell lymphoma in a mesenteric lymph node shows diffuse and strong positive membrane immunoreactivity for B220 antibody. (B) T-cell lymphoma in mesenteric lymph node shows diffuse membrane and cytoplasmic immunoreactivity to CD3 antibody. (C) Histiocytic sarcoma in the liver shows strong and diffuse membrane immunoreactivity to F4/80 antibody. (D-F) The majority of neoplasms had an immunophenotype of T-cell rich, B-cell lymphomas, characterized by a dominant population of neoplastic B cells immunoreactive to B220 antibody (D), with a minority population of well-differentiated T-

cells immunoreactive to CD3 antibody (E), and only a few resident macrophages illustrated by F4/80 immunoreactivity (F). (A-F) 40X, bar = 20um. (G) Distribution, based on immunohistochemistry, of lymphomas collected from *Mlh1*$^{+/+}$ mice treated with sham-, γ-, or ^{56}Fe ion irradiation. (H) Distribution, based on immunohistochemistry, of lymphomas collected from *Mlh1*$^{+/-}$ mice treated with sham-, γ-rays, or ^{56}Fe ion irradiation. IHC was performed on 8–12 lymphomas of *Mlh1*$^{+/+}$ origin and 15–31 lymphomas of *Mlh1*$^{+/-}$ origin.

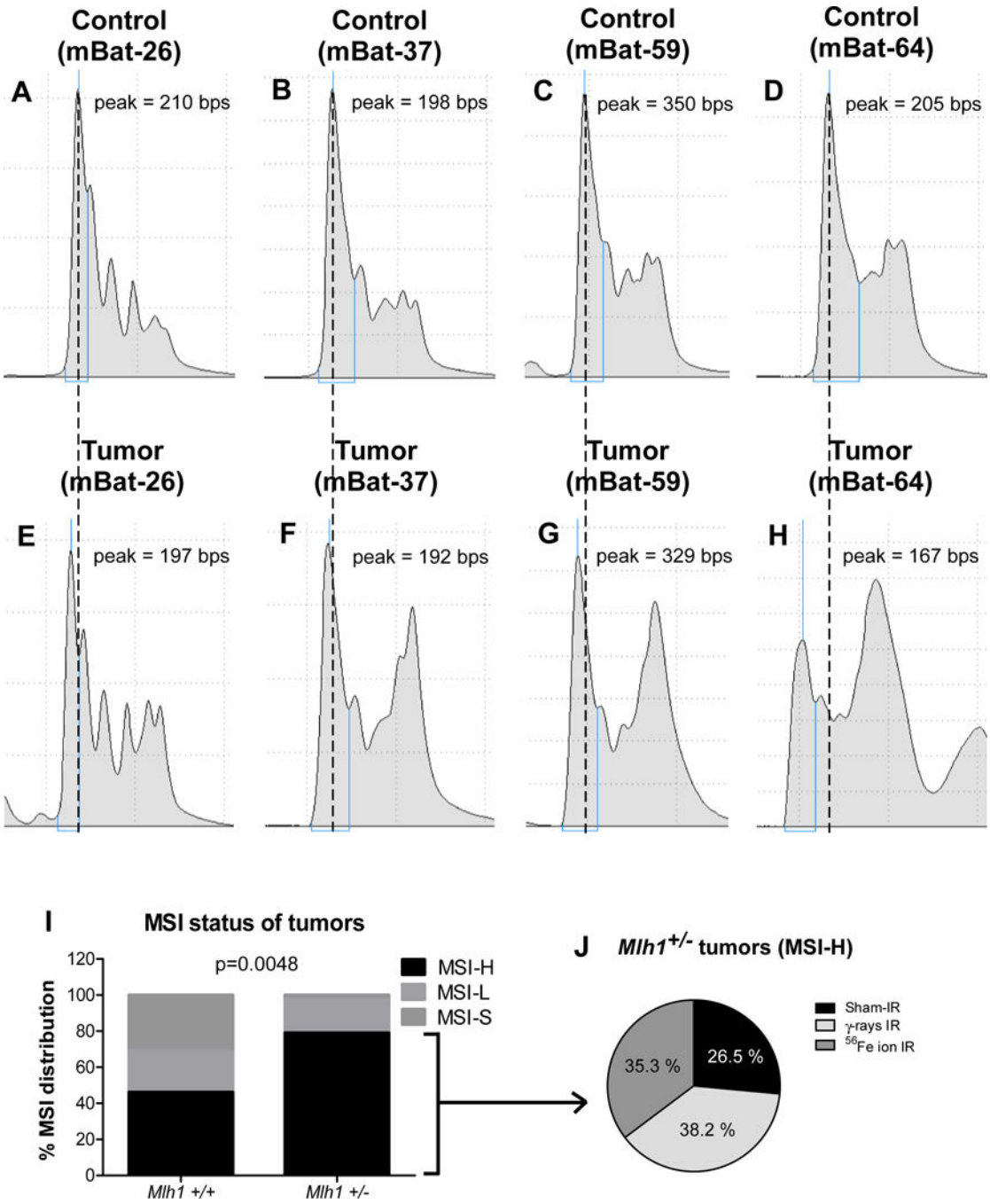

Figure 4: Microsatellite instability found in *Mlh1*$^{+/+}$ and *Mlh1*$^{+/-}$ tumors.

Stable MSI (MSI-S) was found in control tissue (*Mlh1*$^{+/+}$) via the markers mBat-26 (A), mBat-37 (B), mBat-59 (C), and mBat-64 (D). Similarly, high MSI (MSI-H) was observed in *Mlh1*$^{+/-}$ tumor sample also via mBat-26 (E), mBat-37 (F), mBat-59 (G), and mBat-64 (H). MSI distribution in *Mlh1*$^{+/+}$ vs *Mlh1*$^{+/-}$ tumors (I). MSI-H distribution found in tumors of irradiated *Mlh1*$^{+/-}$ mice (J). Number of *Mlh1*$^{+/+}$ and *Mlh1*$^{+/-}$ tumors used for the analysis were 15 and 43, respectively. Distributions were tested using Chi-square tests.

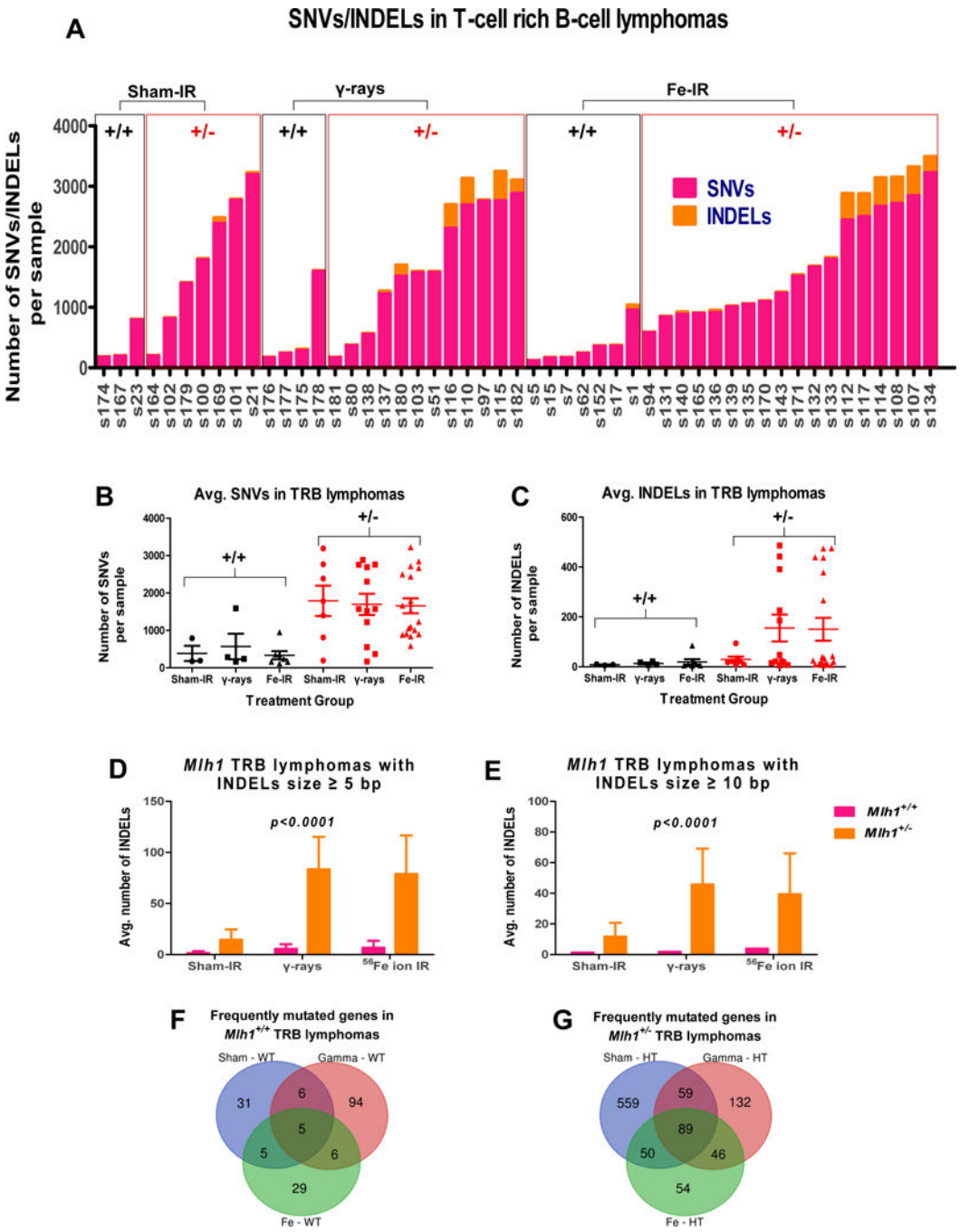

Figure 5: WES analysis of *Mlh1*$^{+/+}$ and *Mlh1*$^{+/-}$ TRB lymphomas.

(A) Number of SNVs and INDELs found in each TRB lymphoma arising from sham- (n = 3 and 7 for *Mlh1*$^{+/+}$ and *Mlh1*$^{+/-}$, respectively), γ-rays (n = 4 and 12 for *Mlh1*$^{+/+}$ and *Mlh1*$^{+/-}$, respectively), or ^{56}Fe ion irradiation (n = 7 and 12 for *Mlh1*$^{+/+}$ and *Mlh1*$^{+/-}$, respectively). (B) Average number of SNVs per *Mlh1*$^{+/+}$ and *Mlh1*$^{+/-}$ cohorts. (C) Average number of INDELs per *Mlh1*$^{+/+}$ and *Mlh1*$^{+/-}$ cohorts. (D) Size of INDELs ≥ 5 bp in each cohort of *Mlh1*$^{+/+}$ and *Mlh1*$^{+/-}$ TRB lymphomas. (E) Size of INDELs ≥ 10 bp in each cohort of *Mlh1*$^{+/+}$ and *Mlh1*$^{+/-}$ TRB lymphomas. Venn Diagram shows number of frequently mutated

genes found in (F) *Mlh1*$^{+/+}$, and (G) *Mlh1*$^{+/-}$ cohorts. P values were determined by a two-way ANOVA model. Data plotted are means ± SEM.

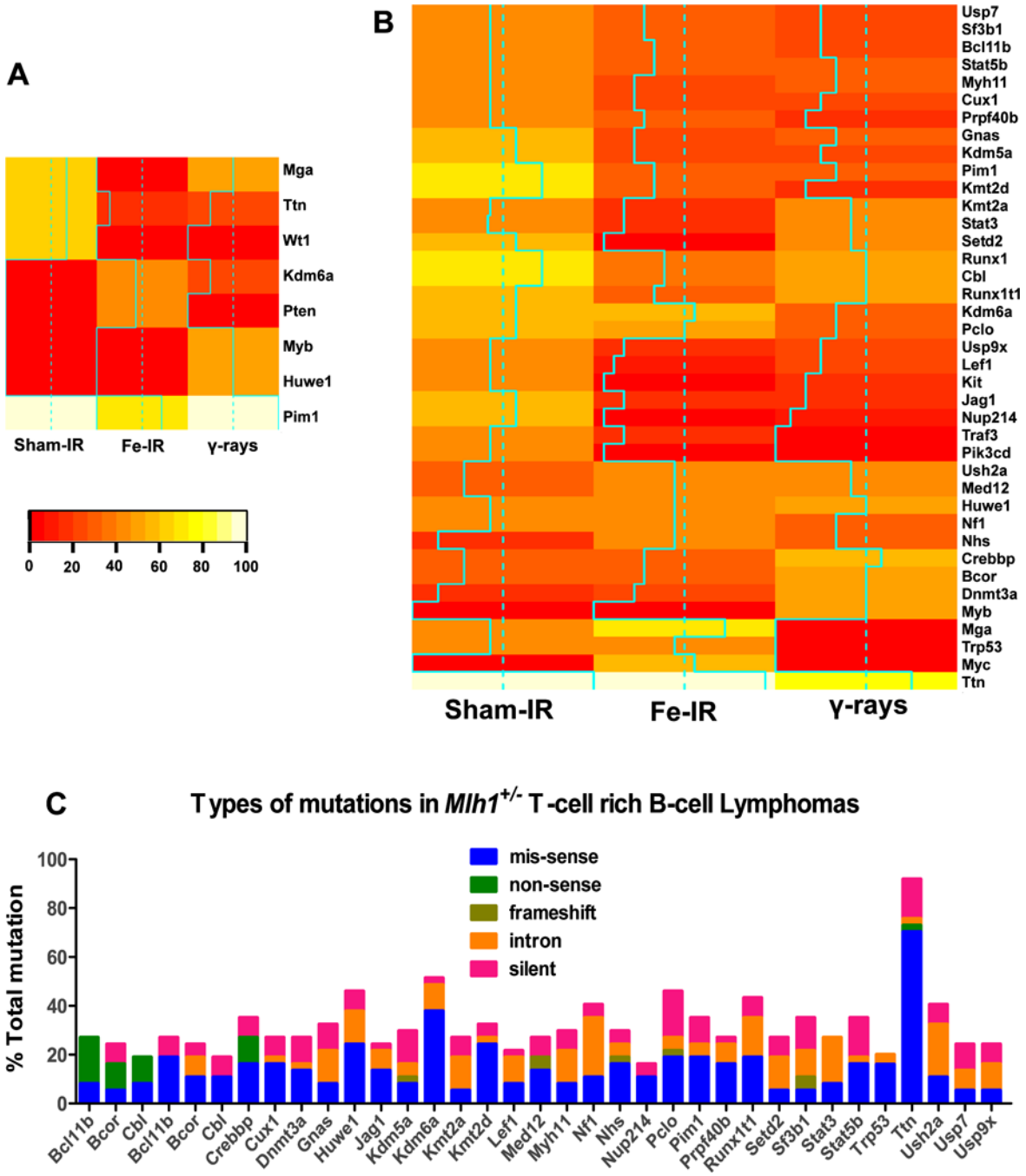

Figure 6: Correlation between frequently mutated mouse TRB lymphoma genes vs human leukemia genes.

Heatmap represents human leukemia genes also found to be frequently mutated in (A) *Mlh1*$^{+/+}$, and (B) *Mlh1*$^{+/-}$ mouse TRB lymphoma cohorts. Solid aqua lines in each Heatmap represent actual mutational frequency of a gene in that particular cohort. (C) Different types of mutations (mis-sense, non-sense, frameshift, intron, and silent) found in each gene of *Mlh1*$^{+/-}$ TRB lymphomas.